

Finite temperature coupled cluster theories for extended systems

Felix Hummel*

*Institute for Theoretical Physics, TU Wien,
Wiedner Hauptstraße 8-10/136, 1040 Vienna, Austria*

E-mail: felix.hummel@tuwien.ac.at

Abstract

At zero temperature, coupled cluster theory is widely used to predict total energies, ground state expectation values and even excited states for molecules and extended systems. However, for systems with a small band gap, such as metals, the zero-temperature approximation not necessarily holds. Thermal effects may even give rise to interesting chemistry on metal surfaces. Most approaches to temperature dependent electronic properties employ finite temperature perturbation theory in the Matsubara frequency formulation. Computations require a large number of Matsubara frequencies to yield sufficiently accurate results, especially at low temperatures.

This work, and independently the work of White and Chan,¹ proposes a coupled cluster implementation directly in the imaginary time domain on the compact interval $[0, \beta]$, closely related to the thermal cluster cumulant approach of Mukherjee and coworkers.²⁻⁴ Here, the arising imaginary time dependent coupled cluster amplitude integral equations are solved in the linearized direct ring doubles approximation, also referred to as Tamm–Dancoff approximation with second order (linearized) screened exchange. In this framework, the transition from finite to zero temperature is uniform and comes at no extra costs, allowing to go to temperatures as low as room temperature.

In this approximation, correlation grand potentials are calculated over a wide range of temperatures for solid lithium, a metallic system, and for solid silicon, a semiconductor.

1 Background

The many-body Schrödinger equation for the electrons in matter can only be solved approximately for systems having more than one electron. Many approximation methods exist, ranging from fast methods providing low accuracy, such as orbital-free density functional theory, to slow methods providing high accuracy, such as full configuration interaction quantum Monte Carlo. Coupled cluster methods provide relatively high accuracy at computational costs that scale only polynomially with the size of the system to be calculated.^{5,6} Although the scaling is still steep, modern computer facilities enable coupled cluster calculations for systems large enough to extrapolate to the infinite size of a solid or a surface.⁷ Moreover, coupled cluster methods offer a whole hierarchy of approximations having increasing accuracy with increasing computational costs. Within this hierarchy, coupled cluster singles doubles with perturbative triples (CCSD(T)) is regarded accurate enough for most practical purposes, providing an accuracy of about 1 kcal/mol or roughly 40 meV/atom.⁸

Coupled cluster methods are well-proven for the zero-temperature case where the underlying starting point calculation, a Hartree–Fock or density functional theory calculation, is non-degenerate. For molecules the energy spectrum is discrete and gapped, making a zero-temperature method a valid approximation. Degeneracies can still occur and they may need to be treated fully quantum-mechanically, as done by multi reference methods. There are various forms of coupled cluster theories for this case. The methods are, however, not as settled as in the non-degenerate closed-shell case and are thus subject to ongoing research, but not scope of this work.⁹ Metallic systems, on the other hand, have a dense energy spectrum such that they interact with their decoherent environment even at the lowest energy scales. They need to be treated by a theory capable of describing their decoherent state

being a mixture, rather than a superposition of pure quantum mechanical states.

At zero temperature the electrons of matter assume the state of lowest possible energy. At finite temperature the many-body quantum system of electrons can be found in any of its states. At thermal equilibrium the probability of finding it in an eigenstate with energy E_n is proportional to the Boltzmann factor $e^{-\beta E_n}$, where $\beta = 1/k_B T$ denotes the inverse temperature of the system.¹⁰ If the system can exchange electrons with the bath in addition to energy, it can also be found in states with fewer or more electrons than suggested, say, by the number of protons N . Thus, a many-body electronic system at finite temperature can be computed by, first, calculating the relevant many-body states $|\Psi_n\rangle$ with a zero-temperature theory which is able to yield excited states, and then determine the finite temperature many-body system by the mixture of states $|\Psi_n\rangle$ with probabilities proportional to their respective Boltzmann factor $e^{-\beta E_n}$.

1.1 Correlating large systems at finite temperature

For large systems, and particularly for metals, the number of relevant excited states quickly becomes unmanageable for practical purposes. Furthermore, conducting the zero temperature coupled cluster calculations is difficult at best for metallic systems due to (quasi) degeneracies of the uncorrelated mean-field description, such as Hartree–Fock (HF) or density functional theory (DFT), serving as the starting point of coupled cluster theories. Alternatively, one can already start from a thermal mean-field description, where each single-body level p forms an independent fermionic system occupied with a probability f_p , and add correlation by means of a finite temperature many-body theory. It is the scope of this work to translate zero temperature coupled cluster theories $CC(T = 0)$ to a finite-temperature starting point, circumventing the difficulties of the first approach arising in large and metallic systems. For systems, where zero temperature coupled cluster can be readily applied, such as insulating systems, thermalizing and adding correlation should commute in the limit of exact correlation theories, as laid out in FIG. 1. For $T \rightarrow 0$ it would even be desirable

that a finite-temperature correlation theory agrees with its zero-temperature counterpart, irrespective of its accuracy, in the non-degenerate case where the zero-temperature coupled cluster theory can be applied.

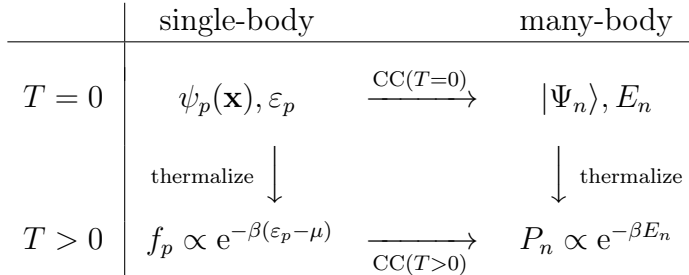


Figure 1: Thermalizing the single-body description and adding correlation by a finite temperature coupled cluster formulation should agree with adding correlation at zero temperature and thermalizing the resulting many-body states in cases where both methods are applicable.

1.2 Imaginary time formulation

The framework employed by finite temperature many-body perturbation theory (MBPT) provides the means of adding correlation to a thermalized starting point. In Appendix A it is briefly outlined and according to Eq. (45) therein, a given term of the perturbation expansion of n th order is calculated by evaluating contractions $\langle \dots \overbrace{\hat{c}_a \dots \hat{c}_b^\dagger} \dots \rangle_0$ of the perturbations \hat{H}_1 at n distinct imaginary times τ_1, \dots, τ_n , integrating the times in an ordered fashion on the interval $0 < \tau_1 < \dots < \tau_n < \beta$. Between the times of the perturbations, say τ_1 and τ_2 , the system propagates according to the mean-field description, namely $\exp\{-(\tau_2 - \tau_1)(\hat{H}_0 - \mu\hat{N})\}$. This is analogous to the time dependent formulation of zero temperature many-body perturbation theory, Wick rotated to imaginary time about the Fermi energy $\varepsilon_F = \mu$. In the zero temperature MBPT the times are integrated on the infinite interval $-\infty < \tau_1 < \dots < \tau_n = 0$. The terms of the many-body expansion are otherwise identical and can in particular be depicted by the same diagrams. The respective evaluation scheme is summarized in FIG. 2. Note, however, that there are diagrams with vanishing contribution at zero temperature but not at finite temperature.



| T | τ integration | $\langle \hat{c}_a \hat{c}_b^\dagger \rangle_0$ | diagrams |
|-------|---------------------------------------------------------------------------------------|-------------------------------------------------|-------------------------------------------------------------------------------------|
| $= 0$ | $\int_{-\infty < \tau_1 < \dots < \tau_{n-1} < \tau_n = 0} d\tau_1 \dots d\tau_{n-1}$ | $\delta_a^b \theta(\varepsilon_a - \mu)$ |  |
| > 0 | $-\frac{1}{\beta} \int_{0 < \tau_1 < \dots < \tau_n < \beta} d\tau_1 \dots d\tau_n$ | $\delta_a^b f^a$ |  |

Figure 2: The many-body perturbation expansion at zero and at finite temperature can be given in terms of the same diagrams, differing only in the way contractions are evaluated and imaginary times τ are to be integrated. The dashed lines indicate $\tau = 0$ and β , respectively. The dotted line denotes minus infinity. $f^a = (1 - f_a)$.

The zero temperature coupled cluster formalism can be stated as a recipe to generate terms of the many-body perturbation expansion. The expansion becomes more and more complete as one goes up in the hierarchy of coupled cluster approximations. Thus, zero temperature coupled cluster theories can be generalized to finite temperature by translating their many-body expansion terms according to FIG. 2.

1.3 Related work

The generalization of Wick's theorem to mixtures, rather than pure Slater determinants, is the key to finite temperature many-body perturbation theory. It was brought forward by Matsubara.^{11,12} Finite temperature was introduced to mean-field theories shortly after, first to Hartree–Fock¹³ and then to density functional theory.¹⁴ Being relatively fast, finite temperature Hartree–Fock and DFT are widely used for *ab-initio* calculations and subject to ongoing research.¹⁵ Second order finite temperature Møller–Plesset theory includes correlation beyond DFT. It is, however, divergent in the low temperature, large system size limit for metals.¹⁶ Many theories exist employing Dyson-like recursion schemes to go to infinite order in the perturbation. The finite temperature random phase approximation (RPA) has been used to study the warm electron gas.^{17–20} RPA corresponds to the direct term of the direct ring approximation of coupled cluster doubles.²¹ Self consistent Green's function methods²²

and dynamical mean field theory (DMFT)^{23,24} solve a coupled set of Dyson-like of equations and have been applied to realistic systems.

The above methods are formulated in the Matsubara frequency domain, which requires knowledge of the symmetry factors of the included diagrams to avoid multiple counting.²⁵ On the other hand, the recursion recipe of coupled cluster theory generates diagrams of all kinds of symmetry, prohibiting any frequency domain and requiring strict (imaginary) time ordering. Hermes *et al.*²⁶ employed a steady-state *ansatz* for coupled cluster doubles within their renormalized perturbation theory²⁷ and apply it to study the Peierls transition in one dimensional infinite hydrogen chains.

Mukherjee and coworkers have rigorously generalized the coupled cluster *ansatz* by working within particularly contracted terms as a chosen *ansatz*, termed thermal cluster cumulant method.²⁻⁴ Translating terms of the formal many-body perturbation expansion shows that this *ansatz* is well-justified. The authors solve this equation for model systems, here a method is presented to solve it for *ab-initio* Hamiltonians of extended systems. Independently of this work, White and Chan¹ propose using the same imaginary time dependent formulation as proposed herein. The authors implement full coupled cluster singles doubles and study the warm uniform electron gas at different densities and temperatures.

Finally, fractional occupancy formulations of coupled cluster theories^{28,29} use the same generalization of Wick's theorem to mixtures as the one employed by finite temperature many-body perturbation theory. However, they usually cannot be viewed as the zero-temperature limit of the grand canonical finite-temperature formalism, as outlined in Subsection 4.2 and discussed in detail in Santra and Schirmer.¹⁶

1.4 Structure of this work

Section 2 gives an imaginary time dependent formulation of zero temperature coupled cluster theories, which also defines a subset of the many-body perturbation expansion. Section 3 translates the subset using the framework of finite temperature many-body perturbation

theory. In Section 4 an algorithm is given to solve the occurring equations for *ab-initio* Hamiltonians. Section 5 applies finite temperature linearized direct ring coupled cluster doubles to solid lithium and silicon to demonstrate its applicability to metals and its convergence behavior for low temperatures. Appendix A gives a brief derivation of finite temperature many-body perturbation theory.

2 Imaginary time dependent zero temperature coupled cluster

This section applies the coupled cluster *ansatz* first to the stationary, then to the (imaginary) time dependent Schrödinger equation. Both formulations yield equivalent results at zero temperature, however, the latter can be used in a finite-temperature framework where one needs to find the imaginary time propagator $\exp\{-\beta\hat{H}\}$ to the point β in imaginary time.

2.1 The coupled cluster *ansatz*

Coupled cluster theories start from a mean-field Hartree–Fock or DFT calculation. Let $\psi_p(\mathbf{x})$ be the spin orbitals of the mean-field Hamiltonian \hat{H}_0 and let $|\Phi\rangle$ denote the Slater determinant of the ground state, where the lowest N orbitals are occupied by the N electrons present in the system. At zero temperature we will use the letters i, j, k, \dots to label occupied orbitals, a, b, c, \dots to label virtual orbitals and p, q, r, \dots to label general spin orbitals. Coupled cluster chooses an exponential *ansatz* acting on the mean-field Slater determinant for the approximation of the many-body wave function

$$|\Psi\rangle = e^{\hat{T}}|\Phi\rangle. \tag{1}$$

The cluster operator \hat{T} is expanded in excitation levels

$$\hat{T} = \hat{T}_1 + \hat{T}_2 + \dots = \sum_{ai} T_i^a \hat{t}_i^a + \sum_{abij} T_{ij}^{ab} \hat{t}_{ij}^{ab} + \dots \quad (2)$$

with the excitation operators $\hat{t}_i^a = \hat{c}_a^\dagger \hat{c}_i$, $\hat{t}_{ij}^{ab} = \hat{c}_a^\dagger \hat{c}_b^\dagger \hat{c}_j \hat{c}_i$, \dots , and with the scalar arrays T_i^a , T_{ij}^{ab} , \dots to be determined, which are referred to as singles, doubles, \dots amplitudes, respectively. This choice ensures multiplicative separability of the approximate many-body wave function for non-interacting subsystems by construction. In the projection coupled cluster method the amplitudes are determined by inserting Eq. (1) into the stationary Schrödinger equation $\hat{H}|\Psi\rangle = E|\Psi\rangle$, left-multiplying it with $\exp\{-\hat{T}\}$ and projecting onto excited Slater determinants $\langle\Phi|\hat{t}_a^i$, $\langle\Phi|\hat{t}_{ab}^{ij}$, \dots , giving

$$0 = \langle\Phi|\hat{t}_a^i e^{-\hat{T}} \hat{H} e^{\hat{T}}|\Phi\rangle, \quad 0 = \langle\Phi|\hat{t}_{ab}^{ij} e^{-\hat{T}} \hat{H} e^{\hat{T}}|\Phi\rangle, \quad \dots \quad (3)$$

In practice, the excitation level is truncated at a given level, say at the doubles level, and the first and the second equations are used to solve for the singles and doubles amplitudes, respectively. The truncation level determines the quality of the approximation. Having found the amplitudes, the above equation is projected onto the ground state Slater determinant $\langle\Phi|$ to yield the coupled cluster ground state energy E in the respective approximation

$$E = \langle\Phi|e^{-\hat{T}} \hat{H} e^{\hat{T}}|\Phi\rangle. \quad (4)$$

The expectation values of Eqs. (3, 4) are evaluated by summing over all fully contracted terms occurring in the expansions according to Wick's theorem. It turns out that only terms of the positive exponential remain where all occurring operators are connected by the contractions, denoted by an apostrophe on the expectation value brackets $\langle\cdot\rangle'$. The operator

equation for determining the doubles amplitudes reads for instance

$$0 = \langle \Phi | \hat{t}_{ab}^{ij} \hat{H} e^{\hat{T}} | \Phi \rangle' \quad (5)$$

and the expansion of the remaining exponential now terminates since the number of the contractions which can be connected to \hat{H} and \hat{t} is finite for a given excitation level of the amplitudes. The energy expression is also simplified by regarding only connected terms to

$$E = \langle \Phi | \hat{H} e^{\hat{T}} | \Phi \rangle'. \quad (6)$$

2.2 Defining time dependent amplitudes

In the finite temperature many-body formalism one is required to compute a density operator $\hat{\rho} \propto \exp\{-\beta\hat{H}\}$. This is equivalent to the time evolution operator from zero to the finite point β in imaginary time. We start by obtaining equations for the amplitudes of the zero-temperature cluster operator $\hat{T}(\tau) = T_i^a(\tau)\hat{\tau}_i^a + T_{ij}^{ab}(\tau)\hat{\tau}_{ij}^{ab}$ which are valid for arbitrary imaginary times τ , rather than just for the stationary case. We insert the coupled cluster approximation for the wave function $\exp\{\hat{T}(\tau)\}|\Phi\rangle$ into the imaginary time dependent Schrödinger equation, giving

$$-e^{\hat{T}(\tau)} \frac{\partial}{\partial \tau} \hat{T}(\tau) |\Phi\rangle = \hat{H} e^{\hat{T}(\tau)} |\Phi\rangle \quad (7)$$

since all excitation operators $\hat{\tau}_i^a, \hat{\tau}_{ij}^{ab}, \dots$ commute with each other. Left-multiplying the above equation with $\exp\{-\hat{T}(\tau)\}$ and projecting onto excited Slater determinants yields differential equations for the amplitudes, reading for the doubles for instance

$$-\frac{\partial}{\partial \tau} T_{ij}^{ab}(\tau) = \langle \Phi | \hat{\tau}_{ab}^{ij} \hat{H} e^{\hat{T}(\tau)} | \Phi \rangle', \quad (8)$$

where only the remaining connected terms are given, as in the case of Eq. (5). Comparing Eq. (8) and Eq. (5) shows that the original coupled cluster amplitudes are the steady-state solution of the imaginary time dependent amplitudes.

2.3 Example: direct ring coupled cluster doubles

In order to give concrete working equations, the amplitudes can be truncated at a certain excitation level. Truncating already at the level of doubles still results in cumbersome equations. We further restrict the considered contractions to those contractions, where all fermionic loops have length 2. The resulting theory is termed direct ring coupled cluster doubles theory (drCCD) or, alternatively, random phase approximation (RPA) with second order screened exchange (SOSEX).^{30,31} Though it does not fully regard fermionic exchange relations, it shares two important qualities of a fully featured coupled cluster singles doubles (CCSD) theory, where all contractions are regarded: a non-linear nature of the amplitude equations and the ability to describe metallic systems in the thermodynamic limit.³² The calculations in Section 5 are all conducted in its linearized approximation. For simplicity, we use the canonical set of creation and annihilation operators, such that $\hat{H}_0 = \sum_p \varepsilon_p \hat{c}_p^\dagger \hat{c}_p$. The Hamiltonian is written in the form $\hat{H} = \hat{H}_0 - \hat{V}_{\text{eff}} + \hat{V}$ with the electron-electron and the effective interaction of the reference given by

$$\hat{V} = \frac{1}{2} \sum_{pqrs} V_{sr}^{pq} \hat{c}_p^\dagger \hat{c}_q^\dagger \hat{c}_r \hat{c}_s, \quad \hat{V}_{\text{eff}} = \sum_{pq} v_q^p \hat{c}_p^\dagger \hat{c}_q, \quad (9)$$

respectively. Hartree–Fock-type terms will only be considered at first order, in accordance with RPA+SOSEX calculations in the literature.^{31,33}

Integrating Eq. (8) with the boundary condition $\hat{T}(\tau \rightarrow -\infty) = 0$ and evaluating all considered contractions, one finally obtains the drCCD equations in algebraic form, free of

any operators:

$$T_{ij}^{ab}(\tau) = (-1) \int_{-\infty < \tau' < \tau} d\tau' e^{-(\tau-\tau')\Delta_{ij}^{ab}} \left[V_{ij}^{ab} + V_{id}^{al} T_{lj}^{db}(\tau') + V_{cj}^{kb} T_{ik}^{ac}(\tau') + V_{cd}^{kl} T_{ik}^{ac}(\tau') T_{lj}^{db}(\tau') \right] \quad (10)$$

$\forall abij$ and implying a sum over all other indices. In this formulation the electron-electron interaction V_{ij}^{ab} and the amplitudes T_{ij}^{ab} are not antisymmetrized. The eigenenergy difference is denoted by $\Delta_{ij}^{ab} = \varepsilon_a + \varepsilon_b - \varepsilon_i - \varepsilon_j$. The drCCD amplitude equations can also be stated in terms of (non-antisymmetrized) Goldstone diagrams

$$\tau \begin{array}{c} \downarrow \downarrow \\ \text{---} \\ \tau' \end{array} = \begin{array}{c} \downarrow \downarrow \\ \text{---} \\ \tau' \end{array} + \begin{array}{c} \downarrow \downarrow \\ \text{---} \\ \tau' \end{array} + \begin{array}{c} \downarrow \downarrow \\ \text{---} \\ \tau' \end{array} + \begin{array}{c} \downarrow \downarrow \\ \text{---} \\ \tau' \end{array}, \quad (11)$$

depicting the contractions and the time-ordered unperturbed propagations from τ' to τ . The imaginary time dependent formulation of the amplitude equations is not the standard formulation, it is, however, readily generalized to finite temperature. Inserting the steady-state *ansatz* $T_{ij}^{ab}(\tau') = T_{ij}^{ab}(\tau) = T_{ij}^{ab}$ into Eq. (10) and integrating over all time differences $0 < \tau - \tau' < \infty$ yields the standard form of the drCCD amplitude equations for non-degenerate systems

$$T_{ij}^{ab} = \frac{V_{ij}^{ab} + V_{id}^{al} T_{lj}^{db} + V_{kj}^{cb} T_{ik}^{ac} + V_{cd}^{kl} T_{ik}^{ac} T_{lj}^{db}}{-\Delta_{ij}^{ab}}. \quad (12)$$

The equations are non-linear and contain the left-hand-side quantity T in contracted forms on the right-hand-side, which can be solved by iteration until convergence is reached. Once the steady-state amplitudes T_{ij}^{ab} are found, the drCCD energy E can be computed by considering all non-vanishing contractions in Eq. (6), eventually retrieving

$$E = \varepsilon_i - v_i^i + \frac{1}{2} (V_{ij}^{ij} - V_{ji}^{ij}) + \frac{1}{2} (V_{ab}^{ij} - V_{ab}^{ji}) T_{ij}^{ab} \quad (13)$$

implying a sum over all indices. The term involving the amplitudes is referred to as drCCD correlation energy, the remaining term is the Hartree-exchange energy E_{HX} .

3 Finite temperature coupled cluster

The connected and fully contracted expectation value giving the zero temperature coupled cluster energy in Eq. (6) corresponds to a subset of the zero temperature many-body perturbation expansion¹. The truncated amplitude equations in the Dyson-like form, as for instance in Eq. (11), define a recursive rule how to generate terms of the perturbation expansion by connecting sub-terms with a finite maximum number of open connections to a more complex sub-term with the same finite maximum number of open connections. The sub-terms are connected by the application of the perturbation. CCSD, for instance, considers all possible connections of the sub-terms with each other having at most four open connections. All open connections are going upwards, so the perturbations occur in (imaginary) time ordered fashion. The number of connections is always even and they come in particle/hole pairs since the perturbation preserves the number of electrons. The sub-terms are connected in topologically distinct ways, such that a single MBPT term, here denoted by a Goldstone diagram, will be evaluated exactly once or not at all. Truncating the cluster operator at higher and higher levels considers more and more open connections of the sub-terms, approaching the full many-body perturbation expansion.

One can therefore generalize coupled cluster to finite temperature by translating the perturbation expansion from zero temperature to finite temperature, as outlined in FIG. 2. At finite temperature the imaginary times of each occurring perturbation are integrated over the finite domain $[0, \beta]$, rather than over the infinite domain of the zero-temperature case. The last perturbation at τ_n also needs to be integrated, rather than being kept fixed. Furthermore, the contractions within quantum mechanical expectation values of the Hartree–Fock or DFT Slater determinant $\langle \Phi | \dots \hat{c}_a \hat{c}_b^\dagger \dots | \Phi \rangle_0$ are superseded by contractions within the ensemble average of the respective finite-temperature mixture. Each single-particle level of the Hartree–Fock or DFT calculation must be allowed to exchange its electron with the

¹The expansion is only considered formally to identify the function returning the energy from the electron repulsion integrals, the eigenenergies, and the ensemble parameters. Individual terms may diverge.

bath if the occupation probabilities are to be independent of each other, enforcing the grand canonical ensemble. In the canonical basis the (non-normalized) density operator factorizes into

$$\hat{\rho}_0 = e^{-\beta(\hat{H}_0 - \mu\hat{N})} = \bigotimes_p e^{-\beta(\varepsilon_p - \mu)\hat{n}_p} \quad (14)$$

with $\hat{n}_p = \hat{c}_p^\dagger \hat{c}_p$ and the fixed chemical potential of the environment μ . The probability of occupation f_p of a single level p is then given by the Fermi–Dirac distribution

$$f_p = \langle \hat{n}_p \rangle_0 = \frac{\text{Tr}\{\hat{\rho}_0 \hat{n}_p\}}{\text{Tr}\{\hat{\rho}_0\}} = \frac{e^{-\beta(\varepsilon_p - \mu)}}{1 + e^{-\beta(\varepsilon_p - \mu)}} \quad (15)$$

and the probability of vacancy of the level p is denoted by $f^p = 1 - f_p$. Matsubara generalized Wick’s theorem to mixtures^{11,12} allowing contractions to be defined for a thermal Hartree–Fock or DFT reference:

$$\langle \dots \overline{\hat{c}_i^\dagger \hat{c}_j} \dots \rangle_0 = \delta_j^i f_i, \quad \langle \dots \overline{\hat{c}_a \hat{c}_b^\dagger} \dots \rangle_0 = \delta_a^b f^a. \quad (16)$$

Products of occupation or vacancy probabilities are denoted by $f_{ij\dots}^{ab\dots} = f^a f_i f^b f_j \dots$, where lower and upper indices are referred to as thermal hole and thermal particle levels, although all indices i, a, \dots are to be summed, in principle, over all single-body levels p . In practice, however, the sum over thermal holes i and thermal particles a can be restricted to levels where f_i and f^a is non-negligible, respectively. The fact that thermal hole indices i and thermal particle indices a can refer to the same level p spawns contractions which are not present in the usual zero-temperature formalism, in which hole and particle states are disjoint. This lays the fundament for finite temperature many-body perturbation theory, in fact, including Hartree–Fock itself, defining the exchange free energy. Appendix A lists a brief derivation of finite temperature many-body perturbation theory. Finite temperature Hartree–Fock and DFT are discussed in.^{13–15}

In the case where the Hartree–Fock or the DFT reference is degenerate in the zero-

temperature limit, diagrams with states that are holes as well as particles remain with non-vanishing contributions. In the degenerate case the zero-temperature limit of the grand canonical ensemble at constant chemical potential does not agree with the zero-temperature theory with a fixed number of electrons. This is referred to as the Kohn–Luttinger conundrum³⁴ and it is treated in detail in Santra and Schirmer.¹⁶

3.1 Finite temperature coupled cluster equations

Translating the MBPT terms means working with the fully contracted operators, rather than with the operators itself. Rather than defining a cluster operator \hat{T} , we define how operators must occur within the fully contracted expectation values of an MBPT term. They are required to have both contractions going upwards, towards positive times:

$$\langle (\cdot) \overbrace{T_i^a \hat{c}_a^\dagger \hat{c}_i} \rangle'_0 = \Downarrow, \quad \langle (\cdot) \overbrace{T_{ij}^{ab} \hat{c}_a^\dagger \hat{c}_b^\dagger \hat{c}_j \hat{c}_i} \rangle'_0 = \Downarrow\Downarrow. \quad (17)$$

Some contractions may no longer vanish at finite temperature, so all of them have to be reconsidered. The algebra of contractions is, however, identical, most importantly

$$\langle (\cdot) \overbrace{\hat{c}_a^\dagger \hat{c}_i \hat{c}_b^\dagger \hat{c}_j} \rangle'_0 = + \langle (\cdot) \overbrace{\hat{c}_b^\dagger \hat{c}_j \hat{c}_a^\dagger \hat{c}_i} \rangle'_0. \quad (18)$$

Thus, the differential equations for the amplitude scalars, as for instance Eq. (8), also hold in the finite temperature case. The equation for the doubles amplitudes reads for instance

$$-\frac{\partial}{\partial \tau} T_{ij}^{ab}(\tau) = \langle \overbrace{\hat{c}_i^\dagger \hat{c}_j^\dagger \hat{c}_b \hat{c}_a} \overbrace{(\hat{H} e^{\hat{T}(\tau)})} \rangle'_0, \quad (19)$$

where no contractions among the \hat{T} s are allowed according to the requirement stated in Eq. (17). Hartree–Fock-type contractions of \hat{H}_1 with itself are, however, allowed.

Having solved the imaginary time dependent amplitudes for all times τ between 0 and β , the coupled cluster grand potential can be computed from the grand potential of the

reference Ω_0 and a reference thermal expectation value of all connected and fully contracted coupled cluster terms with the perturbation part \hat{H}_1

$$\Omega = \Omega_0 - \frac{1}{\beta} \int_0^\beta d\tau \langle \overline{\hat{H}_1 (e^{\hat{T}(\tau)})} \rangle'_0, \quad (20)$$

according to Eq. (45). Also here, contractions of \hat{H}_1 with itself are allowed, contractions among \hat{T} s are not. Note that in the grand canonical ensemble the expectation value of the number operator $\langle \hat{N} \rangle$ will be affected by correlation. In principle, the chemical potential μ needs to be scanned for the value μ_N , such that $\langle \hat{N} \rangle$ is fixed to the desired number of electrons N :

$$\left. \frac{\partial \log \mathcal{Z}(\beta, \mu)}{\beta \partial \mu} \right|_{\mu=\mu_N} = N. \quad (21)$$

The differences $\mu_N - \mu_{N-1}$ and $\mu_{N+1} - \mu_N$ correspond to the finite-temperature generalization of the ionization potential (IP) and the electron affinity (AE), respectively.

3.2 Example: direct ring coupled cluster doubles

The concrete working equations of a zero temperature coupled cluster theory, formulated in imaginary time as in Eq. (10), can be translated to finite temperature by

- extending hole and particle states to overlapping thermal hole and particle states,
- convolving with the time evolution operator $e^{-(\tau-\tau')\Delta_{ij\dots}^{ab\dots}}$ over the finite domain $[0, \tau]$,
and
- multiplying with the thermal occupancies $f_{k\dots}^{c\dots}$ for each contracted thermal particle/hole index.

Applied to the direct ring coupled cluster doubles theory, we obtain

$$T_{ij}^{ab}(\tau) = (-1) \int_0^\tau d\tau' e^{-(\tau-\tau')\Delta_{ij}^{ab}} \left[V_{ij}^{ab} + f_l^d V_{id}^{al} T_{lj}^{db}(\tau') \right. \\ \left. + f_k^c V_{cj}^{kb} T_{ik}^{ac}(\tau') + f_{kl}^{cd} V_{cd}^{kl} T_{ik}^{ac}(\tau') T_{lj}^{db}(\tau') \right] \quad (22)$$

for the doubles amplitudes, implying a sum over all indices occurring only on the right-hand-side. Having solved for the imaginary time dependent amplitudes, the direct ring coupled cluster doubles grand potential is evaluated by

$$\Omega = \Omega_{\text{HX}} + \overbrace{\left[\text{diagram 1} + \text{diagram 2} \right]} = \Omega_{\text{HX}} + \frac{1}{\beta} \int_0^\beta d\tau \left[\frac{1}{2} f_{ij}^{ab} (V_{ab}^{ij} - V_{ab}^{ji}) T_{ij}^{ab}(\tau) \right]. \quad (23)$$

Ω_{HX} denotes the DFT Hartree–Exchange grand potential

$$\Omega_{\text{HX}} = f_i(\varepsilon_i - \mu) + \frac{1}{\beta}(f_i \log f_i + f^i \log f^i) - f_i v_i^i + \frac{1}{2} f_{ij} (V_{ij}^{ij} - V_{ji}^{ij}). \quad (24)$$

4 Solving the finite temperature amplitude equations

At zero temperature only the steady-state solution of the amplitudes is required, while in the finite-temperature case the free energy is determined from averaging over all imaginary times $[0, \beta]$. In the finite-temperature case one indeed needs to solve the system of coupled integral equations (22) to an extent permitting sufficient accuracy in the quadrature of Eq. (23). The system of equations is non-linear and can thus only be solved iteratively, representing the amplitudes on an imaginary time grid, which is not necessarily equidistant. Which choice of the grid points provides sufficient accuracy depends on the system and on the temperature $1/\beta$ of the calculation. The amplitude integral equations can be solved on the grid one-by-one, starting at $T_{ij}^{ab}(\tau_0 = 0) = 0$ and with a guess for $T_{ij}^{ab}(\tau_1)$ at the end of the first interval. From amplitudes at the beginning and at the end of the current

interval a continuous interpolation to arbitrary imaginary times $T(\tau')$ can be constructed and inserted into the right-hand-side of the amplitude equations to be solved, e.g. Eq. (22). Integrating the amplitude equations from the beginning to the end of the interval, employing the interpolation on the r.h.s., gives an updated guess for the amplitudes at the end of the interval $\tilde{T}(\tau_1)$, which should agree with the initial amplitudes $T(\tau_1)$. From the deviation of $\tilde{T}(\tau_1)$ from $T(\tau_1)$ new amplitudes are estimated at τ_1 . Once convergence is reached the next interval can be solved. This procedure only requires storing the amplitudes at the beginning and the end of the current interval and convergence accelerating techniques, such as direct inversion of iterative subspace (DIIS) can be employed.³⁵⁻³⁷ However, the overall accuracy depends strongly on the choice of grid points and the amplitudes must be well-converged at each grid point to minimize error accumulation.

4.1 Linearized direct ring coupled cluster

Neglecting quadratic and higher order terms of the coupled cluster amplitude equations leaves a linear, though inhomogeneous system of equations, which can be solved by diagonalization. Once obtained, the imaginary time dependence of the amplitudes can be evaluated and integrated analytically. In the particular case of the linearized direct ring approximation the matrix is small enough such that diagonalization is computationally feasible. We will therefore employ this approximation to study temperatures as low as room temperature.

The linearized direct ring coupled cluster amplitude equations are given by

$$\begin{aligned}
 T_{ij}^{ab}(\tau) = \tau \text{ [diagram]} &= \tau' \text{ [diagram]} + \text{ [diagram]} + \text{ [diagram]} \\
 &= (-1) \int_0^\tau d\tau' e^{-(\tau-\tau')\Delta_{ij}^{ab}} \left[V_{ij}^{ab} + f_k^c V_{ic}^{ak} T_{kj}^{cb}(\tau') + f_l^d V_{dj}^{lb} T_{il}^{ad}(\tau') \right] \quad (25)
 \end{aligned}$$

Inserting the amplitudes into Eq. (23) gives the expansion of the grand potential in the linearized drCCD approximation. In this approximation the left and the right particle/hole

pairs do not interact and their propagation can be factorized. A particle/hole pair in the states c, k at τ_1 can propagate independently of the other pair into the states b, j at the later time τ_2 . The propagation can be either free or via one or more electron-electron interactions. It can be given by the following Dyson-like equation

$$\begin{aligned}
G_{jc}^{bk}(\tau_2, \tau_1) &= \text{Diagram 1} = \text{Diagram 2} + \text{Diagram 3} \\
&= \delta_c^b \delta_j^k e^{-(\tau_2 - \tau_1) \Delta_j^b} - \int_{\tau_1}^{\tau_2} d\tau' e^{-(\tau_2 - \tau') \Delta_j^b} g_{jl}^{bd} V_{jd}^{bl} G_{lc}^{dk}(\tau', \tau_1), \quad (26)
\end{aligned}$$

where $g_{jl}^{bd} = (f_{jl}^{bd})^{1/2}$ denotes the square roots of the Wick contraction weights. The square roots of the contraction weights are assigned to each leg of the electron-electron interaction in order to retain a symmetric form of the propagator, satisfying

$$\int_{\tau_1}^{\tau_2} d\tau' e^{-(\tau_2 - \tau') \Delta_j^b} g_{jl}^{bd} V_{jd}^{bl} G_{lc}^{dk}(\tau', \tau_1) = \int_{\tau_1}^{\tau_2} d\tau' G_{jd}^{bl}(\tau_2, \tau') g_{kl}^{cd} V_{lc}^{dk} e^{-(\tau' - \tau_1) \Delta_k^c}. \quad (27)$$

Identifying the left two indices of G in Eq. (26) as the row index, and the right two indices as the column of a matrix \mathbf{G} , the particle/hole propagation is given by the matrix exponent

$$\mathbf{G}(\tau_2, \tau_1) = \exp\{-(\tau_2 - \tau_1) \mathbf{A}\} \quad (28)$$

with the effective particle/hole interaction

$$A_{jc}^{bk} = \delta_c^b \delta_j^k (\varepsilon_b - \varepsilon_j) + g_{jk}^{bc} V_{jc}^{bk}. \quad (29)$$

This corresponds to a generalization of the Casida equation in the Tamm–Dancoff approximation to finite temperature.^{21,38} The matrix \mathbf{A} is hermitian permitting an eigendecomposition with real eigenvalues

$$A_{jc}^{bk} = \delta_c^b \delta_j^k \Delta_j^b + g_{jk}^{bc} V_{jc}^{bk} = U_{jF}^b \Lambda_F^F U_k^{*cF}, \quad (30)$$

implying a sum over the eigenvalue index F . The particle/hole imaginary time evolution operator is then given by

$$G_{jc}^{bk}(\tau_2, \tau_1) = U_{jF}^b e^{-(\tau_2 - \tau_1)\Lambda_F^F} U_{kF}^{*cF}. \quad (31)$$

Finding the eigenvalue decomposition scales as $\mathcal{O}(N_v^3 N_o^3)$ with the number of thermal holes N_o and particles N_v , which is of the same order as zero temperature coupled cluster doubles.

Having found the eigenvalue decomposition, one can evaluate the linearized direct ring coupled cluster doubles amplitudes at the time τ by propagating the left and the right particle/hole pairs from the initial electron-electron interaction V_{kl}^{cd} at τ' to the time τ

$$T_{ij}^{ab}(\tau) = (-1) \int_0^\tau d\tau' G_{ic}^{ak}(\tau, \tau') G_{jd}^{bl}(\tau, \tau') g_{kl}^{cd} V_{kl}^{cd}. \quad (32)$$

The correlation contribution to the grand potential in the linearized direct ring coupled cluster doubles approximation is then found to be

$$\begin{aligned} \Omega - \Omega_{\text{HX}} &= \text{[Diagram 1]} + \text{[Diagram 2]} = \frac{1}{\beta} \int_0^\beta d\tau \frac{1}{2} g_{ij}^{ab} (V_{ab}^{ij} - V_{ab}^{ji}) T_{ij}^{ab}(\tau) \\ &= - \left(\frac{1}{\Lambda^{FG}} + \frac{e^{-\beta\Lambda^{FG}} - 1}{\beta(\Lambda^{FG})^2} \right) \frac{1}{2} (W_{FG} - X_{FG}) W^{FG} \end{aligned} \quad (33)$$

with $\Lambda^{FG} = \Lambda_F^F + \Lambda_G^G$ and where W and X denote the direct and the exchange electron-electron interaction in the eigenmodes of the particle/hole propagator, respectively

$$W_{FG} = U_{kF}^c U_{lG}^d g_{kl}^{cd} V_{cd}^{kl}, \quad X_{FG} = U_{kF}^c U_{lG}^d g_{lk}^{cd} V_{cd}^{lk}. \quad (34)$$

A sum over all repeated indices on the right-hand-side is implied and $W^{FG} = \overline{W_{FG}}$. Note that the initial and the final interaction also need to carry the square root of the contraction weights. Computing other observables than the grand potential requires derivatives of the log-partition function with respect to β or μ , according to Appendix A.6. They have to

be computed numerically, as the square roots of the Fermi weights occur in the effective particle/hole interaction \mathbf{A} to be diagonalized.

For finite β the above expression will be finite, also for terms with vanishing eigenvalues. However, degenerate states having non-vanishing probability of both, occupancy as well as of vacancy, need to be treated specially. For such states p, q, r, s (being not necessarily all distinct) the effective particle/hole interaction A_{sr}^{pq} of Eq. (29) will be proportional to the electron-electron interaction V_{sr}^{pq} since all eigenenergies are the same and $g_{sq}^{pr} = g$ is constant. For $p \neq s$, two distinct rows $(p, s) \neq (s, p)$ in the matrix \mathbf{A} will be identical in the case of real-valued orbitals:

$$A_{sr}^{pq} = g V_{sr}^{pq} = g V_{pr}^{sq} = A_{pr}^{sq}. \quad (35)$$

This will render $N_d(N_d - 1)/2$ eigenvalues of \mathbf{A} zero for a group of N_d degenerate states serving equally as particles and as holes. This means that the amplitudes have more degrees of freedom than there is information taken into account for their propagation. However, in the case of real-valued orbitals the matrix of the initial electron-electron interaction $g V_{qr}^{sq}$ in Eq. (32) is also identical to that of the particle/hole effective interaction A_{sr}^{pq} for degenerate states p, q, r, s . Therefore, eigenmodes F of \mathbf{A} with an eigenvalue of zero (purely within the degenerate space) also also have zero coupling to the initial electron-electron interaction and can be disregarded.

4.2 Zero temperature limit

The limit of vanishing temperature or infinite β requires to distinguish between cases where the unperturbed reference is non-degenerate and where it is degenerate. In the non-degenerate case, the matrix \mathbf{A} will be positive definite, having only positive eigenvalues Λ_F^F . The correlation grand potential in the linearized drCCD of Eq. (33) can thus be evaluated in the limit $\beta \rightarrow \infty$ arriving at the zero-temperature expression for the linearized direct ring coupled cluster doubles energy, evaluated from solving the Casida equation in the Tamm–Dancoff

approximation²¹

$$\Omega - \Omega_{\text{HX}} = -\frac{1}{2} \frac{(W_{FG} - X_{FG}) W^{FG}}{\Lambda^{FG}}. \quad (36)$$

In the presence of a finite gap of the occupied and the virtual states there will be no correlation contribution to the expectation value of the number operator since μ can be varied without affecting the correlation contribution to the log-partition function. Thus, the above equation will also be the correlation energy of the zero temperature linearized direct ring coupled cluster doubles approximation.

In the case of N_d degenerate states at the Fermi level in the limit of $T \rightarrow 0$, the matrix \mathbf{A} of the effective particle/hole interaction exhibits $N_d(N_d - 1)/2$ eigenmodes with an eigenvalue of zero. As discussed in the previous section, the initial electron-electron interaction does not couple to these modes and the ldrCCD correlation grand potential also yields a finite value in the degenerate case for $\beta \rightarrow \infty$. However, μ cannot be varied without changing the correlation contribution to the log-partition function. Thus, the zero-temperature limit of the correlation grand potential at the given μ will not yield a zero-temperature correlation energy.

5 Applications

In this section the presented finite temperature coupled cluster framework is applied to solid lithium, a metallic system, and to solid silicon as an insulating system, to demonstrate its practical applicability. All calculations were conducted with the Coupled Cluster for Solids `cc4s` code, developed at TU Wien, based on a density functional theory reference, provided by the Vienna *ab-initio* Simulation Package (VASP).³⁹⁻⁴¹ The linearized direct ring coupled cluster doubles approximation was chosen as a test as it is expected to converge for metallic systems at zero temperature in the thermodynamic limit of an infinite solid. The calculations are not fully converged with respect to the number of virtual orbitals and with respect to the thermodynamic limit. However, the systems provide the respective key features of interest.

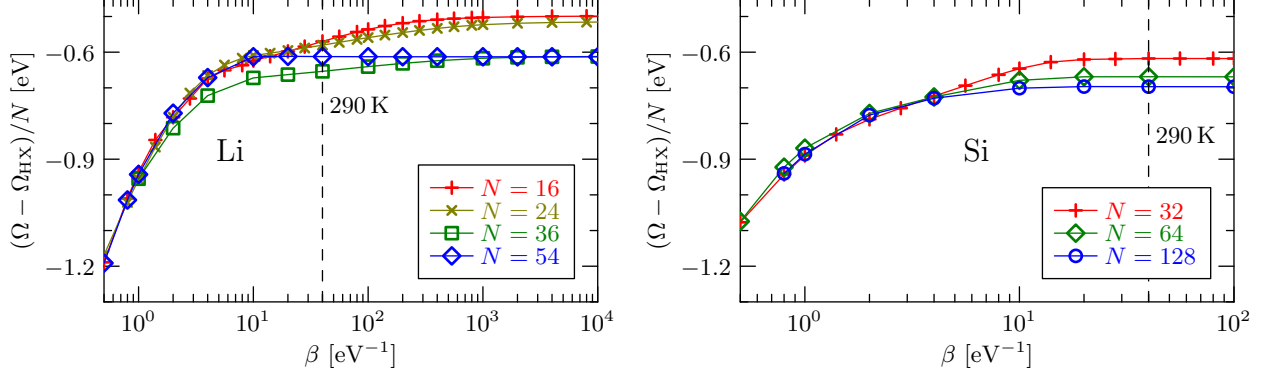


Figure 3: Correlation contribution per electron to the grand potential in the linearized direct ring coupled cluster doubles approximation for solid lithium (Li) and solid silicon (Si) for various system sizes as a function of the inverse temperature β . In the insulating case the correlation grand potential approaches the ground state correlation energy obtained from the zero-temperature theory. In the metallic case the correlation grand potential converges to different values not only due to finite-size errors. Different types of degeneracies at low temperature are expected to give different correlation contributions to the expectation value of the number operator. Only the system with 54 electrons is non-degenerate at low temperatures.

For most system sizes the lithium system is truly degenerate at all temperatures considered. The silicon system provides an underestimated but finite band gap and can therefore also be calculated with the conventional zero temperature linearized direct ring coupled cluster doubles methods, also known as TDA+SOSEX.

The considered lithium super-cells comprise 16, 24, 36, and 54 electrons in approximately 5 restricted orbitals per atom at the Γ -point. The silicon super-cells contain 8, 16, and 32 atoms in approximately 16 restricted orbitals per atom at the Γ -point. Only the valence electrons were contained in the calculations, freezing the He and the Ne core of Li and Si, respectively. All super-cells were relaxed at the k -point-converged DFT level with the Perdew–Burke–Enzerhof (PBE) functional optimized for solids. The kinetic cutoff energy for the calculation of the electron-electron interaction was set to 250 eV. For large systems the diagonalization of the particle/hole effective interaction, given in Eq. (29), poses the most demanding part of the calculation, scaling as $\mathcal{O}(N_v^3 N_o^3)$. The matrix dimensions of the largest considered systems were about 100000×100000 for high temperatures and 25000×25000 for

low temperatures, which is still feasible for standard diagonalization routines, as implemented in ScaLAPACK.

FIG. 3 plots the resulting linearized direct ring coupled cluster doubles (ldrCCD) correlation grand potentials as a function of the inverse temperature β . In the case of the semi-conducting Si, the finite-temperature correlation grand potential approaches the correlation energy, calculated with the existing zero-temperature formalism for the respective system size, as expected. In the case of the metallic Li, the calculations of different sizes converge to different values for low temperatures not only due to finite-size errors. For low temperatures the systems of 16, 24, and 36 atoms exhibit different types of degeneracies at the Fermi edge having 2 electrons in 6 orbitals, 2 electrons in 8 orbitals, and 14 electrons in 8 orbitals. The system of 54 atoms is non-degenerate at low temperatures. The different types of degeneracies lead to different correlation contributions to the grand potential. The correlation contributions to the expectation value of the number operator $\langle \hat{N} \rangle$ are also expected to be different. Twist averaging^{42–44} is expected to improve on the finite-size convergence, however, its implementation into `cc4s` for metallic systems goes beyond the scope of this work.

6 Summary

This work presents a framework for finite temperature coupled cluster theories, including a practical algorithm to apply it to extended systems. In this framework, coupled cluster theories are viewed as rules to generate an (infinite) subset of the finite temperature many-body perturbation expansion. When increasing the truncation level of the cluster operator the subset becomes more and more complete.

For demonstration purposes linearized direct ring coupled cluster doubles correlation grand potentials are calculated for two solids, metallic lithium and semi-conducting silicon. The chosen approximation allows an exact evaluation of the imaginary time behavior by

matrix diagonalization for arbitrarily low temperatures, also for degenerate systems. For all sizes of silicon and for the 54 atom super-cell of lithium the low temperature DFT reference is non-degenerate. The low- but finite-temperature results for these systems can thus be compared with existing non-degenerate zero temperature linearized drCCD results and agreement is found.

Going beyond linearized drCCD requires iterative schemes and a sampling of the imaginary time dependent amplitudes. At high enough temperatures full coupled cluster singles and doubles converges on a uniform grid, as done by White and Chan.¹ Which schemes together with which non-linear approximations allow to go to low temperatures will be subject of future investigation. Certainly, excitations of single electrons, rather than of doubly occupied orbitals, should not be neglected in finite-temperature theories beyond direct ring coupled cluster doubles. Finally, it is worth to remark that derivatives with respect to $\beta = 1/k_B T$ give access to central statistical moments of the *interacting* Hamiltonian, exhibiting properties of the density of states. It remains to be studied how the proposed finite temperature coupled cluster (FT-CC) framework compares to thermalizing the correlated excited states, obtained by an equation of motion coupled cluster (EOM-CC) calculation.^{45,46} The two approaches work fundamentally different: EOM-CC describes correlated excited states by a discrete set of amplitudes for each excited state, while in FT-CC correlation is described by continuous amplitude functions.

Acknowledgements

The author thanks the reviewers for pointing out an error in the original derivation. Fruitful discussions with Andreas Grüneis, Andreas Imler and Joachim Burgdörfer are gratefully acknowledged.

A Brief derivation of finite temperature many-body perturbation theory

This appendix summarizes finite temperature MBPT following the notation of Matsubara's original work.¹¹ It can be found in more detail, for instance in.¹²

In thermal equilibrium, the (non-normalized) density operator $\hat{\rho}$ of the grand canonical ensemble with chemical potential μ is given by

$$\hat{\rho} = e^{-\beta(\hat{H}-\mu\hat{N})}, \quad (37)$$

where $\beta = 1/k_{\text{B}}T$ is the inverse temperature. Applying the Zassenhaus formula separates the density operator into a reference part $\hat{\rho}_0$ and a correlation part \hat{S} :

$$\hat{\rho} = e^{-\beta(\hat{H}_0+\hat{H}_1-\mu\hat{N})} = \underbrace{e^{-\beta(\hat{H}_0-\mu\hat{N})}}_{\hat{\rho}_0} \underbrace{e^{-\beta\hat{H}_1} e^{+\beta^2/2[\hat{H}_0,\hat{H}_1]} \dots}_{\hat{S}}, \quad (38)$$

since \hat{N} commutes with \hat{H}_0 and \hat{H}_1 .

A.1 Bloch equation

The derivative of $\hat{\rho}$ with respect to β defines an equation of motion for $\hat{\rho}$ as a function of β , referred to as Bloch equation

$$-\frac{\partial\hat{\rho}}{\partial\beta} = (\hat{H} - \mu\hat{N})\hat{\rho}. \quad (39)$$

Inserting Eq. (38) on both sides and using $-\partial\hat{\rho}_0/\partial\beta = (\hat{H}_0 - \mu\hat{N})\hat{\rho}_0$ yields

$$-\frac{\partial(\hat{\rho}_0\hat{S})}{\partial\beta} = (\hat{H}_0 - \mu\hat{N})\hat{\rho}_0\hat{S} - \hat{\rho}_0\frac{\partial\hat{S}}{\partial\beta} = (\hat{H}_0 + \hat{H}_1 - \mu\hat{N})\hat{\rho}_0\hat{S}, \quad (40)$$

from which the equation of motion for the correlated part \hat{S} follows

$$-\frac{\partial \hat{S}}{\partial \beta} = \hat{H}_1(\beta) \hat{S}(\beta), \quad (41)$$

with $\hat{H}_1(\tau) = e^{+\tau(\hat{H}_0 - \mu \hat{N})} \hat{H}_1 e^{-\tau(\hat{H}_0 - \mu \hat{N})}$. This is the finite-temperature analog to the interaction picture.

A.2 Perturbation expansion of \hat{S}

The equation of motion for the correlation part \hat{S} can be transformed into a Volterra integral equation with the formal solution

$$\hat{S}(\beta) = \sum_{n=0}^{\infty} (-1)^n \int_{0 < \tau_1 < \dots < \tau_n < \beta} d\tau_1 \dots d\tau_n \hat{H}_1(\tau_n) \dots \hat{H}_1(\tau_1). \quad (42)$$

Note that $\hat{S}(\beta)$ also depends on μ although this is not explicitly denoted.

A.3 Grand potential difference

The grand canonical partition functions of the fully interacting system \mathcal{Z} and of the reference system \mathcal{Z}_0 are given by

$$\mathcal{Z}(\beta, \mu) = \text{Tr}\{\hat{\rho}_0 \hat{S}(\beta)\}, \quad \mathcal{Z}_0(\beta, \mu) = \text{Tr}\{\hat{\rho}_0\} \quad (43)$$

respectively. We are interested in the grand potential difference between the fully interacting and the reference system

$$\Delta\Omega = -\frac{1}{\beta} (\log \mathcal{Z}(\beta, \mu) - \log \mathcal{Z}_0(\beta, \mu)) = -\frac{1}{\beta} \log \langle \hat{S}(\beta) \rangle_0, \quad (44)$$

where $\langle \hat{A} \rangle_0 = \text{Tr}\{\hat{\rho}_0 \hat{A}\} / \mathcal{Z}_0(\beta, \mu)$ denotes the statistical expectation value of the operator \hat{A} in the reference system \hat{H}_0 .

A.4 Linked cluster theorem at finite temperature

The terms in Eq. (42) can be expressed as the exponential of a subset, consisting only of connected (linked) terms.⁴⁷ Thus,

$$\Delta\Omega = -\frac{1}{\beta} \sum_{n=1}^{\infty} (-1)^n \int_{0 < \tau_1 < \dots < \tau_n < \beta} d\tau_1 \dots d\tau_n \langle \hat{H}_1(\tau_n) \dots \hat{H}_1(\tau_1) \rangle'_0, \quad (45)$$

where $\langle \hat{A} \rangle'_0$ denotes the statistical expectation value of \hat{A} in the reference system, restricted to connected Wick contractions only.

A.5 Finite temperature MP2

Given the finite temperature Hartree–Fock (HF) operator and the interacting Hamiltonian in the canonical HF basis

$$\hat{H}_0 = \sum_p \varepsilon_p \hat{c}_p^\dagger \hat{c}_p, \quad (46)$$

$$\hat{H} = \sum_{pq} h_q^p \hat{c}_p^\dagger \hat{c}_q + \frac{1}{2} \sum_{pqrs} V_{sr}^{pq} \hat{c}_p^\dagger \hat{c}_q^\dagger \hat{c}_r \hat{c}_s, \quad (47)$$

Eq. (45) can be evaluated, for instance, up to second order, arriving at finite temperature Møller–Plesset theory for the correlation grand potential

$$\Delta\Omega^{(2)} = - \sum_{abij} \left(\frac{1}{\Delta_{ij}^{ab}} + \frac{e^{-\beta\Delta_{ij}^{ab}} - 1}{\beta(\Delta_{ij}^{ab})^2} \right) \frac{1}{2} f_{ij}^{ab} (V_{ab}^{ij} - V_{ab}^{ji}) V_{ij}^{ab} \quad (48)$$

with the shorthand notations $\Delta_{ij}^{ab} = \varepsilon_a + \varepsilon_b - \varepsilon_i - \varepsilon_j$,

$$f_p = \frac{e^{-\beta(\varepsilon_p - \mu)}}{1 + e^{-\beta(\varepsilon_p - \mu)}}, \quad f^p = 1 - f_p, \quad (49)$$

and $f_{ij}^{ab\dots} = f^a f_i f^b f_j \dots$. Note that there is, in principle, no distinction between hole and particle indices. For reference Hamiltonians other than Hartree–Fock, expressions can be

found in Ref. 16.

A.6 Thermal expectation values

Derivatives of the log-partition function with respect to β or μ yield central statistical moments of the Hamiltonian \hat{H} and of the number operator \hat{N} , respectively

$$\langle \hat{H} \rangle = \frac{\partial \log \mathcal{Z}(\beta, \mu)}{-\partial \beta} \qquad \langle \hat{N} \rangle = \frac{\partial \log \mathcal{Z}(\beta, \mu)}{\beta \partial \mu} \qquad (50)$$

$$\langle \Delta^2 \hat{H} \rangle = \frac{\partial^2 \log \mathcal{Z}(\beta, \mu)}{(-\partial \beta)^2} \qquad \langle \Delta^2 \hat{N} \rangle = \frac{\partial^2 \log \mathcal{Z}(\beta, \mu)}{(\beta \partial \mu)^2} \qquad (51)$$

and so forth, with $\Delta \hat{A} = \hat{A} - \langle \hat{A} \rangle$.

References

- (1) White, A.; Chan, G. A time-dependent formulation of coupled cluster theory for many-fermion systems at finite temperature. *arXiv preprint arXiv:1807.09961* **2018**,
- (2) Sanyal, G.; Mandal, S. H.; Mukherjee, D. Thermal averaging in quantum many-body systems: a non-perturbative thermal cluster cumulant approach. *Chem. Phys. Lett.* **1992**, *192*, 55–61.
- (3) Sanyal, G.; Mandal, S. H.; Guha, S.; Mukherjee, D. Systematic nonperturbative approach for thermal averages in quantum many-body systems: The thermal-cluster-cumulant method. *Phys. Rev. E* **1993**, *48*, 3373–3389.
- (4) Mandal, S. H.; Ghosh, R.; Sanyal, G.; Mukherjee, D. *Int. J. Mod. Phys. B* **2003**, *17*, 5367–5377.
- (5) Coester, F.; Kümmel, H. Short-range correlations in nuclear wave functions. *Nucl. Phys.* **1960**, *17*, 477–485.

- (6) Čížek, J. In *Advances in Chemical Physics*; LeFebvre, R., Moser, C., Eds.; John Wiley & Sons, Inc., 1969; pp 35–89.
- (7) Gruber, T.; Liao, K.; Tsatsoulis, T.; Hummel, F.; Grüneis, A. Applying the Coupled-Cluster Ansatz to Solids and Surfaces in the Thermodynamic Limit. *Phys. Rev. X* **2018**, *8*, 021043.
- (8) Shavitt, I.; Bartlett, R. J. *Many-body methods in chemistry and physics: MBPT and coupled-cluster theory*; Cambridge University Press: Cambridge; New York, 2009.
- (9) Coughtrie, D. J.; Giereth, R.; Kats, D.; Werner, H.-J.; Köhn, A. Embedded Multireference Coupled Cluster Theory. *J. Chem. Theory Comput.* **2018**, *14*, 693–709, PMID: 29345927.
- (10) Breuer, H.; Petruccione, F. *The Theory of Open Quantum Systems*; Oxford University Press, 2007.
- (11) Matsubara, T. A New Approach to Quantum-Statistical Mechanics. *Prog. Theor. Phys.* **1955**, *14*, 351–378.
- (12) Thouless, D. J. *The quantum mechanics of many-body systems*, second dover edition ed.; Dover Publications, Inc, 2014.
- (13) Mermin, N. Stability of the thermal Hartree-Fock approximation. *Ann. Phys. (N. Y.)* **1963**, *21*, 99 – 121.
- (14) Mermin, N. Thermal Properties of the Inhomogeneous Electron Gas. *Phys. Rev. A* **1965**, *137*, 1441.
- (15) Eschrig, H. *Phys. Rev. B* **2010**, *82*.
- (16) Santra, R.; Schirmer, J. Finite-temperature second-order many-body perturbation theory revisited. *Chem. Phys.* **2017**, *482*, 355–361.

- (17) Gupta, U.; Rajagopal, A. K. Exchange-correlation potential for inhomogeneous electron systems at finite temperatures. *Phys. Rev. A* **1980**, *22*, 2792–2797.
- (18) Perrot, F. Temperature-dependent nonlinear screening of a proton in an electron gas. *Phys. Rev. A* **1982**, *25*, 489–495.
- (19) Perrot, F.; Dharma-wardana, M. W. C. Exchange and correlation potentials for electron-ion systems at finite temperatures. *Phys. Rev. A* **1984**, *30*, 2619–2626.
- (20) Csanak, G.; Kilcrease, D. Photoabsorption in hot, dense plasmas—The average atom, the spherical cell model, and the random phase approximation. *J. Quant. Spectrosc. Radiat. Transf.* **1997**, *58*, 537–551.
- (21) Scuseria, G. E.; Henderson, T. M.; Sorensen, D. C. The ground state correlation energy of the random phase approximation from a ring coupled cluster doubles approach. *J. Chem. Phys.* **2008**, *129*, 231101.
- (22) Welden, A. R.; Rusakov, A. A.; Zgid, D. Exploring connections between statistical mechanics and Green’s functions for realistic systems: Temperature dependent electronic entropy and internal energy from a self-consistent second-order Green’s function. *J. Chem. Phys.* **2016**, *145*.
- (23) Metzner, W.; Vollhardt, D. Correlated Lattice Fermions in $d = \infty$ Dimensions. *Phys. Rev. Lett.* **1989**, *62*, 324–327.
- (24) Held, K. Electronic structure calculations using dynamical mean field theory. *Adv. Phys.* **2007**, *56*, 829–926.
- (25) Mattuck, R. D. *A Guide to Feynman Diagrams in the Many-Body Problem*; Dover Publications: Mineola, N.Y, 1992.
- (26) Hirata, S.; Hermes, M. R. Finite-temperature coupled-cluster, many-body perturbation, and restricted and unrestricted Hartree–Fock study on one-dimensional solids:

- Luttinger liquids, Peierls transitions, and spin- and charge-density waves. *J. Chem. Phys.* **2015**, *143*, 102818.
- (27) Hirata, S.; He, X. On the Kohn–Luttinger conundrum. *J. Chem. Phys.* **2013**, *138*, 204112.
- (28) Yang, W.; Mori-Sánchez, P.; Cohen, A. J. Extension of many-body theory and approximate density functionals to fractional charges and fractional spins. *J. Chem. Phys.* **2013**, *139*, 104114.
- (29) Margraf, J. T.; Bartlett, R. Communication: Coupled cluster and many-body perturbation theory for fractional charges and spins. *J. Chem. Phys.* **2018**, *148*, 221103.
- (30) Freeman, D. Coupled-cluster expansion applied to the electron gas: Inclusion of ring and exchange effects. *Phys. Rev. B* **1977**, *15*, 5512–5521.
- (31) Grüneis, A.; Marsman, M.; Harl, J.; Schimka, L.; Kresse, G. Making the random phase approximation to electronic correlation accurate. *J. Chem. Phys.* **2009**, *131*, 154115.
- (32) Shepherd, J. J.; Grüneis, A. Many-Body Quantum Chemistry for the Electron Gas: Convergent Perturbative Theories. *Phys. Rev. Lett.* **2013**, *110*, 226401.
- (33) Harl, J.; Schimka, L.; Kresse, G. Assessing the quality of the random phase approximation for lattice constants and atomization energies of solids. *Phys. Rev. B* **2010**, *81*.
- (34) Kohn, W.; Luttinger, J. M. Ground-State Energy of a Many-Fermion System. *Phys. Rev.* **1960**, *118*, 41–45.
- (35) Pulay, P. Convergence acceleration of iterative sequences. the case of scf iteration. *Chem. Phys. Lett.* **1980**, *73*, 393–398.
- (36) Pulay, P. ImprovedSCF convergence acceleration. *J. Comput. Chem.* **1982**, *3*, 556–560.

- (37) Scuseria, G. E.; Lee, T. J.; Schaefer, H. F. Accelerating the convergence of the coupled-cluster approach. *Chem. Phys. Lett.* **1986**, *130*, 236–239.
- (38) Dreuw, A.; Head-Gordon, M. Single-Reference ab Initio Methods for the Calculation of Excited States of Large Molecules. *Chem. Rev.* **2005**, *105*, 4009–4037.
- (39) Blöchl, P. E. Projector augmented-wave method. *Phys. Rev. B* **1994**, *50*, 17953–17979.
- (40) Kresse, G.; Hafner, J. Norm-conserving and ultrasoft pseudopotentials for first-row and transition elements. *J. Phys. Condens. Matter* **1994**, *6*, 8245.
- (41) Kresse, G.; Furthmüller, J. Efficient iterative schemes for ab initio total-energy calculations using a plane-wave basis set. *Phys. Rev. B* **1996**, *54*, 11169–11186.
- (42) Filippi, C.; Ceperley, D. M. Quantum Monte Carlo calculation of Compton profiles of solid lithium. *Phys. Rev. B* **1999**, *59*, 7907–7916.
- (43) Lin, C.; Zong, F. H.; Ceperley, D. M. Twist-averaged boundary conditions in continuum quantum Monte Carlo algorithms. *Phys. Rev. E* **2001**, *64*.
- (44) Holzmann, M.; Clay, R. C.; Morales, M. A.; Tubman, N. M.; Ceperley, D. M.; Pierleoni, C. Theory of finite size effects for electronic quantum Monte Carlo calculations of liquids and solids. *Phys. Rev. B* **2016**, *94*.
- (45) Monkhorst, H. J. Calculation of properties with the coupled-cluster method. *Int. J. Quantum Chem.* **1977**, *12*, 421–432.
- (46) Stanton, J. F.; Bartlett, R. J. The equation of motion coupled-cluster method. A systematic biorthogonal approach to molecular excitation energies, transition probabilities, and excited state properties. *J. Chem. Phys.* **1993**, *98*, 7029–7039.
- (47) Lancaster, T.; Blundell, S. *Quantum field theory for the gifted amateur*, first edition ed.; Oxford University Press: Oxford, 2014.